Nonlinear Amplification and Decay of Phase-Mixed Waves in Compressing Plasma

P. F. Schmit,[1] I. Y. Dodin,[1] J. Rocks,[2] and N. J. Fisch[1]
[1]*Department of Astrophysical Sciences, Princeton University, Princeton, New Jersey 08544, USA*
[2]*Department of Physics, Carnegie Mellon University, Pittsburgh, Pennsylvania 15213, USA*
(Received 10 September 2012; published 28 January 2013)

Through particle-in-cell simulations, we show that plasma waves carrying trapped electrons can be amplified manyfold via compressing plasma perpendicularly to the wave vector. These simulations are the first *ab initio* demonstration of the conservation of nonlinear action for such waves, which contains a term independent of the field amplitude. In agreement with the theory, the maximum of amplification gain is determined by the total initial energy of the trapped-particle average motion but otherwise is insensitive to the particle distribution. Further compression destroys the wave; electrons are then untrapped at suprathermal energies and form a residual beam. As compression continues, the bump-on-tail instability is triggered each time one of the discrete modes comes in resonance with this beam. Hence, periodic bursts of the electrostatic energy are produced until a wide quasilinear plateau is formed.

DOI: 10.1103/PhysRevLett.110.055001 PACS numbers: 52.35.Fp, 47.10.ab, 52.25.−b, 52.65.Rr

Introduction.—Bernstein-Greene-Kruskal (BGK) waves [1] or, more generally, nonlinear plasma waves loaded with autoresonantly trapped electrons, have been studied extensively in literature, as they are generated ubiquitously, e.g., through kinetic instabilities [2] and saturation of collisionless damping [3]. Such waves can also be excited by external fields [4,5] and then affect coupling of these fields with the plasma. In particular, the physics of intense laser-plasma interactions is influenced by the trapped-particle nonlinearity, an issue of immediate practical importance that has been studied vigorously recently [6,7]. It hence has been found that, even on the very basic level, the dynamics of BGK-like waves is still full of surprises. Notwithstanding the existence of well-developed kinetic theories [8,9], which are much-inclusive but also not easily tractable for the same reason, this dynamics is yet to be understood qualitatively in many aspects [10–13]. Maximally reduced models seem advantageous for this purpose [14,15]. In particular, the averaged-Lagrangian theory of Refs. [11–13] renders analytical transparency, while, numerically, one-dimensional (1D) particle-in-cell (PIC) simulations are distinctly enlightening [7,16–18]. Below we combine these tools to explore the dynamics of BGK-like waves in time-evolving plasma, which exhibit a host of interesting paradigmatic phenomena.

We seed a 1D wave as a phase-mixed, periodic BGK-like structure [Fig. 1(a)] in plasma, which then is compressed perpendicularly to the wave vector, k. While k is fixed at transverse compression [19], the frequency, ω, increases, approximately following the increasing plasma frequency, ω_p. Electrons that were trapped initially are then accelerated such that their average velocity remains equal to the phase velocity, $u = \omega/k$ [Fig. 1(b)]. The energy density, W_t, associated with their average motion eventually becomes comparable to the electrostatic energy density in the wave, W_E. Hence, the number of linear plasmons, or the wave linear action [20], is not conserved. However, we show that the *nonlinear* action is conserved as predicted [11,12]. What is remarkable about this nonlinear action for periodic waves is the inclusion of a term independent of the wave amplitude, E. Our work is the first numerical confirmation of this theory, which we use also to explain the observed limit on the maximum W_E attained during compression. Specifically, this maximum depends on W_{t0}/W_{E0} (the index 0 will refer to the initial, uncompressed BGK structure) but otherwise is insensitive to the particle distribution. Further compression destroys the wave; electrons are then untrapped at suprathermal

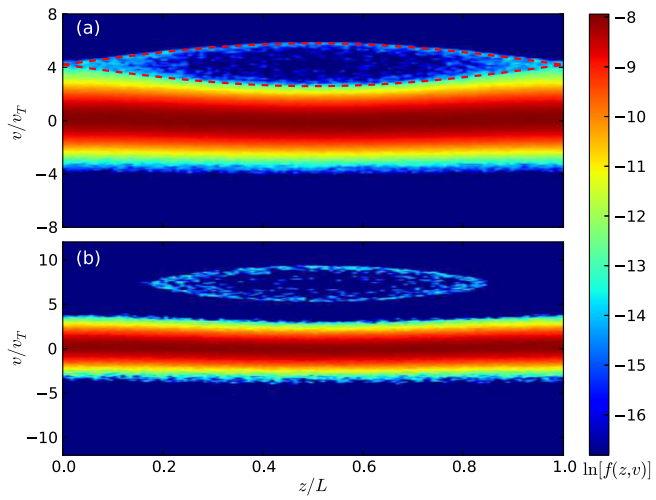

FIG. 1 (color online). Snapshots of typical electron distributions, $f(z, v)$, associated with nonlinear waves in our PIC simulations. (a) The initial, uncompressed BGK structure after the driver is turned off; the dashed red line is the separatrix confining trapped electrons. (b) An adiabatically compressed wave; a phase-space island of trapped electrons has been detached from the bulk plasma via autoresonant acceleration.

energies and form a residual beam. As compression continues, the bump-on-tail instability is triggered each time one of discrete modes comes in resonance with this beam. Hence, periodic bursts of the electrostatic energy are produced until a wide quasilinear plateau is formed. Below we explain these results in more detail.

Numerical model.—Following Ref. [21], we numerically emulate transverse compression by rescaling the mass and charge of PIC particles with time. The charge-to-mass ratio is kept fixed, so rescaling mimics the redistribution of charge across the perpendicularly homogeneous charge sheets modeled by the 1D PIC code. As we take the plasma to be collisionless, the motion parallel to k is thus fully decoupled from the perpendicular motion, so the nature of the compression is inessential; e.g., it can be ballistic or driven by a compressing magnetizing field. Anisotropy-driven instabilities [22], which could invalidate this assumption for some physical systems, are assumed negligible on the compression time scale and are not addressed below. Also, ions are modeled as a uniform charge-neutralizing background, the justification being as in Ref. [17]. Electrons are initialized as a 1D homogeneous Maxwellian distribution with parallel thermal speed v_T, which is approximately conserved during compression. For the longitudinal motion, periodic boundary conditions are imposed along the z axis with period L.

A nonlinear wave is excited by an external potential, $\phi_{\rm ext}(z, t)$, which can be, e.g., a ponderomotive potential, like in Ref. [23]. The difference from Ref. [23], however, is that we take $\phi_{\rm ext}$ to be weak and resonant to the linear Langmuir mode from the beginning, namely, at *fixed* driver frequency $\omega_0 = \omega_{p0}\Omega_0$. Here, $\Omega \doteq (1 + 3\kappa^2)^{1/2} \approx 1$, $\kappa \doteq kv_T/\omega_p$, and $\omega_p^2 \doteq 4\pi ne^2/m$ (the symbol $\doteq$ is used for definitions), with e and m being the electron charge and mass; specifically, in order to change the resonant frequency of the fundamental eigenmode between simulations, we vary ω_{p0} but maintain fixed $k = 2\pi/L$ and v_T. (Note that we choose to operate at the longest resolved wavelength in order to create controlled settings suppressing the coalescence instability [24], and, through that, isolate the effects of our specific interest.) Another distinction from Ref. [23] is that our $\phi_{\rm ext}(z, t)$ is transient, similar to Ref. [5], and is used only for seeding a wave with small initial $\eta \doteq W_t/W$ (Table I); here, $W = 2\Omega^2 W_E$ is the linear wave energy density, and $W_E = E^2/(16\pi)$. After that, the driver is turned off, and the wave evolves self-consistently.

Adiabatic effects.—Except for a minor frequency shift [13], the initial phase-mixed periodic wave is approximately linear, so its early evolution conserves the linear action, $\mathcal{I} = \int_{\mathcal{V}}(W/\omega)d\mathcal{V}$, where $\mathcal{V}$ is the plasma volume [19]. Thus $W/\omega = NW_0/\omega_0$, where $N \doteq n/n_0$ is the compression ratio, and n is the plasma density. Since $\omega \approx \omega_p \propto n^{1/2}$, this results in $G \approx N^{3/2}$ for the amplification gain, $G \doteq W_E/W_{E0}$. At the early stage, $G(N)$ is hence the same as at parallel compression [17]. (Keep in mind that Ref. [17] discusses the wave total energy rather than the energy density, so an extra factor of N must be taken into account when comparing with that paper.) However, since $\kappa \propto n^{-1/2}$ decreases, collisionless damping is now suppressed at all times. This makes transverse compression qualitatively different from longitudinal compression, where induced Landau damping was found earlier to be the dominant limitation on wave amplification, since there $\kappa \propto n^{3/2}$ [17]. For example, in the present study we routinely observe $G \sim 10^2$, and even then no *absolute* limit on G is detected in our model.

TABLE I. Parameters of sample simulations, same as for Figs. 2 and 3. Shown are $M_0 \doteq u_0/v_T$ and $\kappa_0 \doteq kv_T/\omega_{p0}$, together with the associated $\eta_0 \doteq W_{t0}/W_0$, as inferred from direct calculation of W_{t0} and W_{E0} for a given initial state. Also shown is $\delta\eta_0/\eta_0$, which is the relative correction to η_0, as determined by fitting the analytical solution, Eq. (1), to the simulated $G(N)$; here $G \doteq W_E/W_{E0}$, and $N \doteq n/n_0$. The right column shows the initial ratio of the (space-averaged) trapped-electron density and the total density, n_{t0}/n_0.

M_0	κ_0	η_0	$\delta\eta_0/\eta_0$	n_{t0}/n_0
3.8	0.30	0.7909	−17%	14.2×10^{-4}
4.0	0.28	0.5406	−10%	9.70×10^{-4}
4.2	0.26	0.2900	0.01%	5.99×10^{-4}
4.4	0.25	0.1981	2.3%	5.20×10^{-4}
4.8	0.22	0.0721	11%	3.10×10^{-4}
6.0	0.17	0.0055	−8.6%	0.48×10^{-4}

However, since $\kappa \propto n^{-1/2}$ decreases, collisionless damping is now suppressed at all times. This makes transverse compression qualitatively different from longitudinal compression, where induced Landau damping was found earlier to be the dominant limitation on wave amplification, since there $\kappa \propto n^{3/2}$ [17]. For example, in the present study we routinely observe $G \sim 10^2$, and even then no *absolute* limit on G is detected in our model.

For given initial conditions, however, the maximum amplification is still limited, now by nonlinear effects. Note that trapped electrons are accelerated autoresonantly to high energies as their average velocity stays equal to $u \gg v_T$ [Fig. 1(b)]. While their average density, $n_t = Nn_{t0}$, is small, the associated energy density $W_t = n_t mu^2/2$ grows faster than $W_E \propto N^{3/2}$, namely, as $W_t \propto n_t\omega^2 \propto N^2$, so the amplification is eventually halted.

Remarkably, this process can also be described quantitatively in simple terms. First of all, note that trapped electrons do not affect the wave shape appreciably, specifically, if $\omega_t^2 \ll \omega_E^2$ [25]; here, $\omega_t = (n_t/n)^{1/2}\omega_p$ is the trapped-beam frequency, and $\omega_E = (eEk/m)^{1/2}$ is the bounce frequency. Thus, the wave can be considered monochromatic, as we also confirm numerically (to be discussed below). The half-width of the trapping island along the velocity axis, $v_t = k\omega_E$, then grows roughly as $v_t \propto E^{1/2} \propto N^{3/8}$, whereas the island center moves at $u \propto N^{1/2}$. Correspondingly, the island lower boundary, located at velocities $u - v_t \le v < u$, travels *up* in velocity space. This prevents the wave from trapping new electrons from the bulk plasma. In turn, trapping at the upper boundary, $u < v \le u + v_t$, is insignificant, because passing particles are sparse there [Fig. 1(a)]. Thus, the trapped distribution is preserved when the island detaches from the bulk, the error

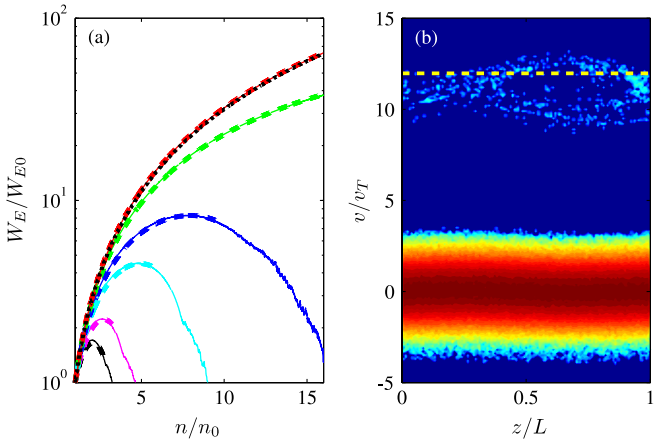

FIG. 2 (color online). (a) Amplification gain vs compression ratio for different $M_0 \doteq u_0/v_T$, in ascending order: $M_0 = 3.8$ (black), 4.0 (magenta), 4.2 (cyan), 4.4 (blue), 4.8 (green), and 6.0 (red). For the remaining parameters, see Table I. Solid lines are results from PIC simulations, smoothed on the time scales ω_E^{-1}. The dashed lines are Eq. (1) with η_0 adjusted to provide the best fit. The dotted line, nearly matching the red curve, is the scaling predicted by the linear action conservation, $G \approx N^{3/2}$. (b) Deteriorating trapped particle island in phase space during wave decay. The dashed line marks the linear phase velocity of the resonant mode, $\omega_p\Omega/k$. Since u exceeds the island average velocity, the wave nonlinear frequency shift is negative, as expected.

in n_t being within few percent in our simulations. Moreover, a gap appears between the separatrix and the trapped population [Fig. 1(b)], whose bounce motion remains adiabatic and, thus, conserves its phase volume even as the ambient island expands.

According to Ref. [11], such a wave, as it is quasiperiodic and evolves slowly, must conserve its nonlinear action, $\mathcal{I}_{\rm NL}$. Assuming that the passing-particle response is approximately linear, one can write $\mathcal{I}_{\rm NL} = \mathcal{I} + \mathcal{I}_t$, where $\mathcal{I}_t = \int(2W_t/\omega)d\mathcal{V}$; see Eq. (52) in Ref. [11]. (In application to homogeneous waves that we consider here, this theorem can as well be understood as conservation of the nonlinear wave canonical momentum [12,20]; also see Ref. [9].) Note two remarkable features of this result. First of all, the conserved quantity is insensitive to the precise shape of the trapped-particle distribution, which would affect $\mathcal{I}_{\rm NL}$ only through the nonlinear frequency shift [13], negligible for our purposes. Second, part of the wave action, $\mathcal{I}_t$, happens to be independent of the wave amplitude, in a drastic variation from how the fundamental physics of nonlinear waves is usually pictured in literature [26]. Using that $\mathcal{I}_{\rm NL} = \mathcal{I}_{\rm NL,0}$, one gets

$$G = (\Omega_0/\Omega)^2(\omega/\omega_0)N[1 - 2\eta_0(\omega/\omega_0 - 1)], \quad (1)$$

or, simply, $G \approx N^{3/2}[1 - 2\eta_0(N^{1/2} - 1)]$. This shows that, up to small nonlinear and thermal corrections, η_0 is *the only* parameter that determines the amplification gain for a given compression ratio N. The maximum gain also can be calculated readily as $G_m = G(N_m)$, where N_m satisfies $G'(N_m) = 0$. Specifically, we find $N_m \approx [3(2 + \eta_0^{-1})/8]^2$, so $G_m \approx 0.013\eta_0^{-3}$.

To compare these formulas with our simulation results, the following tests were performed. First, we inferred η_0 by least-squares fitting of our one-parameter analytical solution to simulated $G(N)$ in the range $1 \le N \lesssim N_m$. For those best-fitted values, $\bar{\eta}_0$, the analytical solution reproduces the numerical curves almost perfectly [Fig. 2(a)]. We then compare $\bar{\eta}_0$ with η_0 obtained by direct calculation of W_{t0} and W_{E0} (Table I). The small deviations, $\delta\eta_0 \doteq \bar{\eta}_0 - \eta_0$, which depend on $M_0 \doteq u_0/v_T$, are explained as follows. At $M_0 \lesssim 3$, relatively many passing electrons are close to the separatrix initially, causing visible nonlinearity of bulk oscillations; although weak, this nonlinearity is yet comparable to the trapped-particle effect, so the function $\mathcal{I}_{\rm NL}(W_{t0}, W_{E0})$ is not quite as simple as taken above. At $M \gtrsim 5$, the bulk nonlinearity is inessential, but the trapped-particle count is small (less than one per grid cell), so the numerical noise becomes an issue. Even so, however, $\delta\eta_0$ is seen to be within few percent, a surprisingly high accuracy for the simple analytical model that we employ. This corroborates our theoretical assumptions and also serves as the first *ab initio* test for the theory proposed in Refs. [11,12].

Nonadiabatic effects.—At $N > N_m$, the wave amplitude decreases, so the separatrix shrinks. Even the adiabatic theory thereby predicts that autoresonant electrons will eventually start to escape the trapping island, at least when G re-approaches unity; this corresponds to the compression ratio of about $16N_m/9$. In reality, however, the wave starts to deteriorate earlier [Fig. 2(b)]. This is caused by the collective instability of the trapped-particle population like those generically described in Ref. [27]. The associated field oscillations [Fig. 3(a) and inset] make the separatrix quiver, at about the bounce frequency, with increasing amplitude. Hence, electrons escape the trapping island stochastically and form a homogeneous beam with velocity $v_b \approx u$. More precisely, the beam velocity is slightly lower than u [Fig. 2(b)]; this is due to the nonlinear frequency shift, which, as predicted [13], we observe to be negative. The wave hence finds itself on the descending slope of the beam distribution $f_b(v)$. Then, Landau damping is triggered, and the wave deteriorates rapidly.

The energy, which the original wave has drawn from the driver and subsequent compression, yet remains stored in the beam. As v_b stays fixed, it is eventually matched by the phase velocities of higher modes, $u_\ell \approx \omega_p L/(2\pi\ell)$, which continue to increase [Fig. 3(b)]. Each $u_{\ell\ge2}$ first approaches v_b from the ascending slope of $f_b(v)$, and, thus, the ℓth mode is amplified from noise through the bump-on-tail instability. (Interestingly, modes with $\ell \ge 2$ can draw even more energy than left by the first mode, since the

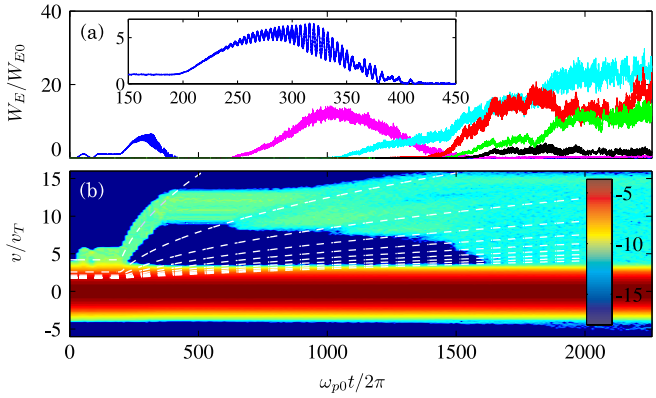

FIG. 3 (color online). Wave evolution for $M_0 = 4.2$ (Table I), up to $N \simeq 100$. (a) Electrostatic energy density vs time for individual eigenmodes with wave numbers (from left to right in terms of initial excitation) $k_\ell = 2\pi\ell/L$: $\ell = 1$ (blue), 2 (magenta), 3 (cyan), 4 (red), 5 (green), and 6 (black). The inset is a close-up of the main figure. (b) Space-averaged velocity distribution, $f(v)$, in a logarithmic scale; the normalization is $\int_{-\infty}^{\infty} f(v)dv = 1$. The white dashed lines are the phase velocities of the first ten eigenmodes ($\ell = 1, \ldots, 10$).

beam density continues to grow due to compression. In this sense, having the original mode to cast once-autoresonant electrons to v_b effectively makes an amplifier out of the plasma, which is powered by mechanical compression). Yet u_ℓ continues to grow, so it then enters the descending slope, and the wave again decays through autoresonant acceleration of trapped electrons and Landau damping. The process is hence repeated by the $(\ell + 1)$th mode, and so on. In a system of finite size L, such as the one considered here, the spectrum discreteness can separate these events in time; then periodic bursts of the electrostatic energy are observed [Fig. 3(a)]. Each resonant mode, however, spreads out the beam somewhat, so a wide quasilinear plateau is formed eventually [Fig. 3(b)]. Hence, compression continues to amplify the residual electrostatic energy, but distinct bursts disappear.

Conclusions.—This is the first study of BGK-like wave dynamics in plasma undergoing compression perpendicularly to the wave vector. A host of interesting phenomena are observed in this paradigmatic problem. First, such compression can amplify a wave manyfold. Second, this amplification conserves the wave nonlinear action, for which our study is the first *ab initio* confirmation. Third, the amplification gain has an upper limit determined by the total initial energy of the trapped-particle average motion but otherwise is insensitive to the particle distribution. Fourth, the electrostatic energy continues to produce bursty behavior even after the original wave has decayed. Apart from the academic interest in these new phenomena and the numerical demonstration of the nonlinear action conservation, the fact that BGK-like waves can be amplified so powerfully suggests new methods of coupling energy into plasma.

This work was supported by the U.S. Defense Threat Reduction Agency, the DOE under Contract No. DE-AC02-09CH11466, and by the NNSA SSAA Program through DOE Research Grant No. DE-FG52-08NA28553. One of us (J. R.) was supported by the Science Undergraduate Laboratory Internships program.

[1] I. B. Bernstein, J. M. Greene, and M. D. Kruskal, Phys. Rev. **108**, 546 (1957); B. Eliasson and P. K. Shukla, Phys. Rep. **422**, 225 (2006); C. S. Ng, A. Bhattacharjee, and F. Skiff, Phys. Plasmas **13**, 055903 (2006).

[2] M. M. Shoucri, Phys. Fluids **22**, 2038 (1979); H. L. Berk, B. N. Breizman, and N. V. Petviashvili, Phys. Lett. A **234**, 213 (1997); Q. Lu, S. Wang, and X. Dou, Phys. Plasmas **12**, 072903 (2005).

[3] R. K. Mazitov, Zh. Prikl. Mekh. Tekh. Fiz. **1**, 27 (1965) [J. Appl. Mech. Tech. Phys. **6**, 22 (1965)]; T. O'Neil, Phys. Fluids **8**, 2255 (1965); G. Manfredi, Phys. Rev. Lett. **79**, 2815 (1997).

[4] B. I. Cohen and A. N. Kaufman, Phys. Fluids **20**, 1113 (1977); H. A. Rose and D. A. Russell, Phys. Plasmas **8**, 4784 (2001); W. Bertsche, J. Fajans, and L. Friedland, Phys. Rev. Lett. **91**, 265003 (2003); R. R. Lindberg, A. E. Charman, and J. S. Wurtele, Phys. Plasmas **15**, 055911 (2008); T. W. Johnston, Y. Tyshetskiy, A. Ghizzo, and P. Bertrand, Phys. Plasmas **16**, 042105 (2009); J. W. Banks, R. L. Berger, S. Brunner, B. I. Cohen, and J. A. F. Hittinger, Phys. Plasmas **18**, 052102 (2011).

[5] F. Valentini, T. M. O'Neil, and D. H. E. Dubin, Phys. Plasmas **13**, 052303 (2006).

[6] H. A. Rose, Phys. Plasmas **12**, 012318 (2005); M. S. Hur, R. R. Lindberg, A. E. Charman, J. S. Wurtele, and H. Suk, Phys. Rev. Lett. **95**, 115003 (2005); J. L. Kline *et al.*, Phys. Plasmas **13**, 055906 (2006); H. X. Vu, D. F. DuBois, and B. Bezzerides, Phys. Plasmas **14**, 012702 (2007); D. J. Strozzi, E. A. Williams, A. B. Langdon, and A. Bers, Phys. Plasmas **14**, 013104 (2007); H. A. Rose and L. Yin, Phys. Plasmas **15**, 042311 (2008); L. Yin, B. J. Albright, K. J. Bowers, W. Daughton, and H. A. Rose, Phys. Plasmas **15**, 013109 (2008); D. Bénisti, D. J. Strozzi, and L. Gremillet, Phys. Plasmas **15**, 030701 (2008); P. E. Masson-Laborde, W. Rozmus, Z. Peng, D. Pesme, S. Hüller, M. Casanova, V. Yu. Bychenkov, T. Chapman, and P. Loiseau, Phys. Plasmas **17**, 092704 (2010).

[7] I. N. Ellis, D. J. Strozzi, B. J. Winjum, F. S. Tsung, T. Grismayer, W. B. Mori, J. E. Fahlen, and E. A. Williams, Phys. Plasmas **19**, 112704 (2012).

[8] V. B. Krapchev and A. K. Ram, Phys. Rev. A **22**, 1229 (1980); T. H. Dupree, Phys. Fluids **25**, 277 (1982); H. Schamel, Phys. Rep. **140**, 161 (1986); J. P. Holloway and J. J. Dorning, Phys. Rev. A **44**, 3856 (1991); H. Schamel, Phys. Plasmas **7**, 4831 (2000); D. Bénisti and L. Gremillet, Phys. Plasmas **14**, 042304 (2007); A. I. Matveev, Fiz. Plazmy **34**, 114 (2008) [Plasma Phys. Rep. **34**, 95 (2008)].

[9] V. L. Krasovskii, Zh. Eksp. Teor. Fiz. **107**, 741 (1995) [JETP **80**, 420 (1995)].

[10] D. Bénisti, O. Morice, and L. Gremillet, Phys. Plasmas **19**, 063110 (2012); P. Khain, L. Friedland, A. G. Shagalov, and J. S. Wurtele, Phys. Plasmas **19**, 072319 (2012); H. Schamel, Phys. Plasmas **19**, 020501 (2012).
[11] I. Y. Dodin and N. J. Fisch, Phys. Plasmas **19**, 012102 (2012).
[12] I. Y. Dodin and N. J. Fisch, Phys. Plasmas **19**, 012104 (2012).
[13] I. Y. Dodin and N. J. Fisch, Phys. Plasmas **19**, 012103 (2012); Phys. Rev. Lett. **107**, 035005 (2011).
[14] R. R. Lindberg, A. E. Charman, and J. S. Wurtele, Phys. Plasmas **14**, 122103 (2007); N. A. Yampolsky and N. J. Fisch, Phys. Plasmas **16**, 072104 (2009); B. N. Breizman, Nucl. Fusion **50**, 084014 (2010).
[15] P. Khain and L. Friedland, Phys. Plasmas **17**, 102308 (2010).
[16] J. E. Fahlen, B. J. Winjum, T. Grismayer, and W. B. Mori, Phys. Rev. Lett. **102**, 245002 (2009).
[17] P. F. Schmit, I. Y. Dodin, and N. J. Fisch, Phys. Rev. Lett. **105**, 175003 (2010).
[18] P. F. Schmit, I. Y. Dodin, and N. J. Fisch, Phys. Plasmas **18**, 042103 (2011).
[19] I. Y. Dodin, V. I. Geyko, and N. J. Fisch, Phys. Plasmas **16**, 112101 (2009).
[20] For a summary and references on linear action conservation, see I. Y. Dodin and N. J. Fisch, Phys. Rev. A **86**, 053834 (2012).
[21] P. F. Schmit and N. J. Fisch, Phys. Rev. Lett. **108**, 215003 (2012).
[22] S. P. Gary and J. Wang, J. Geophys. Res. **101**, 10749 (1996).
[23] L. Friedland, P. Khain, and A. G. Shagalov, Phys. Rev. Lett. **96**, 225001 (2006).
[24] K. V. Roberts and H. L. Berk, Phys. Rev. Lett. **19**, 297 (1967).
[25] V. L. Krasovsky, Phys. Scr. **49**, 489 (1994).
[26] G. B. Whitham, *Linear and Nonlinear Waves* (Wiley, New York, 1974), Chap. 14, 15.
[27] M. V. Goldman, Phys. Fluids **13**, 1281 (1970).